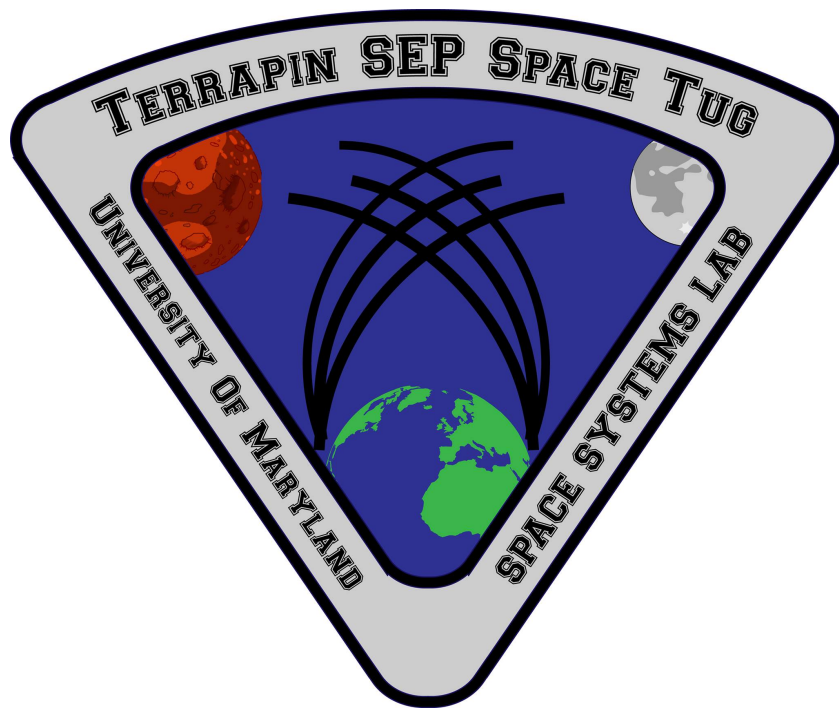


NASA BIG Idea Challenge Technical Paper

A Reusable Modular Solar Electric Propulsion (SEP) Space Tug to Transfer Payloads from Low Earth Orbit (LEO) to Lunar Distant Retrograde Orbit (LDRO)



University of Maryland
Department of Aerospace Engineering

TSST (Terrapin SEP Space Tug) Team Members:

Erich A. Robinson-Tillenburg
Ignacio E. Viciano
Zheng “Jerry” Zhang
Victor A. Meszaros
Ángel Benedicto

Faculty Advisor:

Dr. David Akin

1 SEP Tug Concept Overview

The development of a solar electric propulsion (SEP) Space Tug is a promising step forward in humanity's quest to truly become a space-faring civilization. Ever since Space Electric Rocket Test 1 in 1964, the National Aeronautics and Space Administration has worked tirelessly to advance the technology readiness level of electric propulsion. Why has this technology received so much focus and attention from the brightest minds in the field of space exploration?

The answer is simple, solar electric propulsion space tugs are being developed because they are extremely efficient. Electric propulsion offers vastly greater specific impulse and thus proportionally greater propellant efficiency than chemical propulsion. Thus, while it cannot produce enough thrust to exit the Earth's atmosphere, it offers an ideal transportation system for the inter-orbital transfer of payloads once they have left Earth's atmosphere.

Other than the Dawn Spacecraft, which achieved a peak power of 10kW, solar electric propulsion, as it stands currently, has only operated with power with single digits of kilowatts. This has limited its use to station keeping. With the upcoming Asteroid Robotic Redirect Mission, NASA will demonstrate the viability of a 50kW SEP Tug. Once this has been done it is the goal of NASA to develop and implement SEP tugs in the 100s of kW. Tugs in this power range will allow the timely transfers of large payloads from Low Earth Orbit (LEO) to Lunar Distance Retrograde Orbit (LDRO) and Low Martian Orbit (LMO). This will provide a valuable tool for space exploration as it will significantly reduce the cost of prepositioning assets such as habitats, return vehicles, and construction equipment near the Moon, Mars, and beyond. The goal of this paper is to advance the development of such a Tug and thus bring mankind one step closer to becoming space-faring civilization.

2 TSST Tug Design Overview

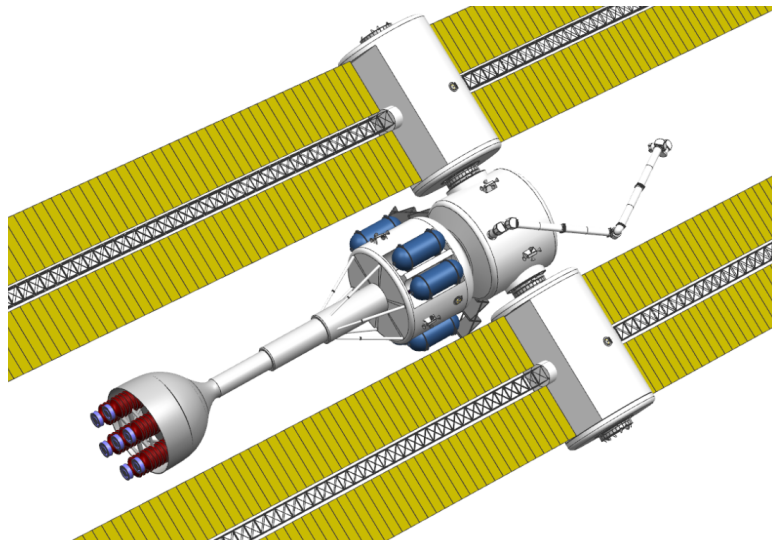


Figure 1: Designed Tug.

The design being proposed is a 200 kW modular, reusable solar electric propulsion (SEP) Space Tug to carry pressurized and unpressurized cargo to and from Low Earth Orbit (LEO) and Lunar Distance Retrograde Orbit (LDRO); with the option to expand to a 500 kW system to travel between LEO and Low Mars Orbit (LMO). In order to improve the economic advantages of such a tug, emphasis has been placed on robotic assembly in orbit, reusability, repairability, and modularity of the tug while maintaining design simplicity.

The designed Tug is comprised of several modules: a central "keystone module", two solar panel modules with the option to add additional solar panel modules, and a propulsion module. An

on-board robotic arm will travel between the modules in a slinky fashion to assist in the assembly of the Tug, berthing of payloads and to allow the transfer of replacement batteries and propellant tanks. The total mass is displayed in Table 1.

Subsystem	Mass (kg)
Hall effect thrusters	1827
Gimbals	914
DDU	92
Xenon feed system	28
Xenon tanks	1003
RCS	356
Solar panels	2669
Batteries	4000
Thermal control system	390
Fairing	800
Avionics	464
Wiring	350
Robotic arm	411
Inert mass	13304

Table 1: Designed Tug mass breakdown.

The keystone module has four docking ports and serves as the connection hub for the solar panel modules, propulsion module, and payload. It contains the avionics, reaction control system, payload support systems, batteries to power the avionics prior to assembly, and a 500 kW rated direct drive power processing unit (DDU). During nominal operation, the on-board robotic arm will be mounted to the keystone module to be used for repairs and an on-board robotic arm will allow for the transfer of propellant tanks as well as assist in the assembly of the Tug.

During nominal operation 200 kW of power will be generated by the two solar power modules connected to either side of the keystone module via vibration isolated, berthing mechanisms with power and data transmission capabilities. There is an additional berthing mechanism on each solar power module so that additional solar power modules can be connected in order to increase the power being generated to 500 kW. This will also enable solar panel modules which have undergone critical failure to be replaced. Each solar power module contains a set of solar panel arrays, voltage converters, and batteries. The solar power modules each have geared, motorized ball bearings such that it can be rotated to allow for pitch control. This system combined with the ability of the Tug to roll about its central axis will allow all of the solar panels to be pointed so that they always face the sun.

The propulsion module consists of a tank module as well as an engine module. It is attached to the keystone module via a vibration isolated, berthing mechanism on top of the tank module that has power and data transfer capability. This detachable connection will enable the propulsion module to be replaced in the event it is outlived by the solar panel module and/or keystone modules increasing both modularity and reusability.

Seven 100 kW Nested Hall Effect Thrusters (NHTs) are contained within the engine module. The power consumption of the NHTs can be adjusted in-flight such that during 200 kW missions to LDRO these engines will run at 28 kW and for 500 kW missions to LMO they can be ramped up to 71 kW. The engine module is then connected to the tank module by a 9 m telescopic boom containing fuel and power lines. It is necessary that the truss structure be expandable as it allows the Tug to be stored in a much smaller configuration during launch in the United Launch Alliance Delta IV M+(4,2) and will prevent low-velocity excess ions from colliding with the tank structure when deployed. The tank module will accommodate three operating Xenon tanks, with fuel necessary for a mission to LDRO, and will be able to carry six extra tanks in order to perform a longer space mission to LMO. Spent tanks will be replaced by new tanks using a "revolver" mechanism which rotates the new tanks inside the structure and remove empty tanks.

The propellant tanks will be delivered to the Tug using a spacecraft with autonomous docking capabilities, such as a Dragon 2, that docks to the keystone module at the same port used for payloads. It is necessary that tank refueling be conducted prior to payload delivery. Tanks will then be connected to the tank module by the on-board robotic arm and a valve system developed as part of the Nitrogen Oxygen Recharge System [1](NORS) by NASA will be used. Adapting the NORS to Xenon propellant tanks will allow propellant tanks to be hot swapped into the engine feed lines. Having a system that allows propellant tanks to be added and removed, as well as engines with variable specific impulse, will allow the Tug to adapt to a wide variety of transit time requirements and be expanded to missions to LMO.

A cost breakdown of the total cost per SEP Tug in 2017 dollars is depicted in Figure 2. This includes the price of launch, nonrecurring and manufacturing costs for one keystone module, one propulsion module loaded with propellant, and two solar power modules each providing 100kW of power. Once each Tug is in orbit it has been designed to complete 10 payload deliveries of 20 MT to LDRO in its 15 year lifetime. Each additional refueling costs \$42 Million and so for the first Tug this totals approximately \$6.5 Billion to deliver 200MT of payload from LEO to LDRO or \$32.5 Million per MT. For the 10th Tug produced this figure drops to approximately \$2.5 Billion for 10 round trips or \$12.5 Million per MT, from LEO to LDRO, over the lifetime of the Tug.

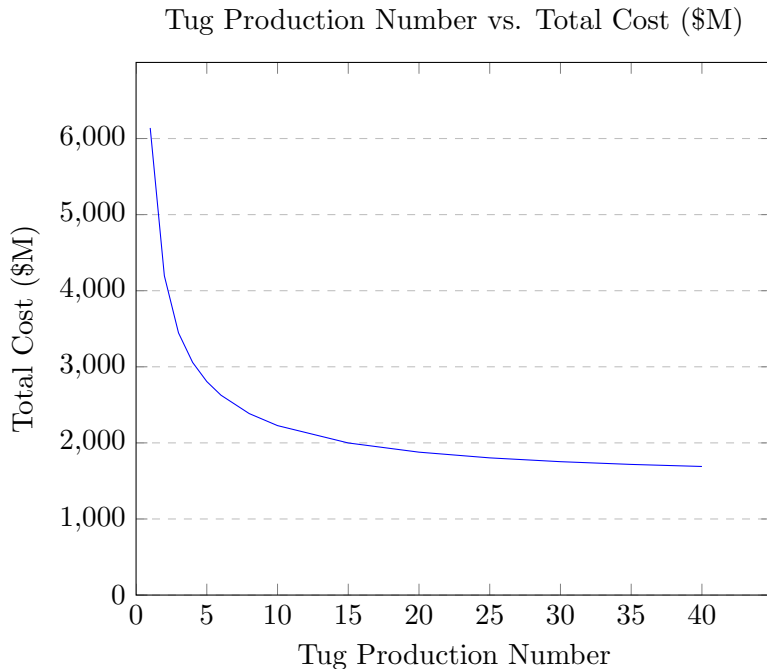


Figure 2: Cost analysis over production time

2.1 Solar Panels

Taking into account radiation, temperature, assembly, shadowing, blocking diodes, and configuration factors, it was determined that approximately 124,000 solar cells would be needed to produce 200 kW during nominal operation. This results in a total approximate solar panel surface area and mass of 1060 m^2 and 2700 kg respectively. The total surface area and mass will be distributed into four solar panels, two in each solar panel module. The power system was developed such that it produces 200 kW of power during the least favorable conditions (not including time spend in shade) the Tug will see during its missions. This occurs when the Tug is in LEO as this orbit has the highest solar panel steady state temperature and the performance of the solar cells is inversely proportional to steady state temperature.

Size and mass calculations were conducted using a 100 V power system as this is what is used on the ISS. Azurspace 3G30C solar cells are used, which are gallium arsenide (GaAs) triple junction cells with a surface area of 120x60 mm and an average efficiency of 29.4% at the Beginning Of Life. These solar cells are flight proven and have a TRL of 9. The Tug will travel an orbit with an inclination of 5.14° (inclination of the Moon relative to Earth), which means a 28.57° inclination with respect to the ecliptic.

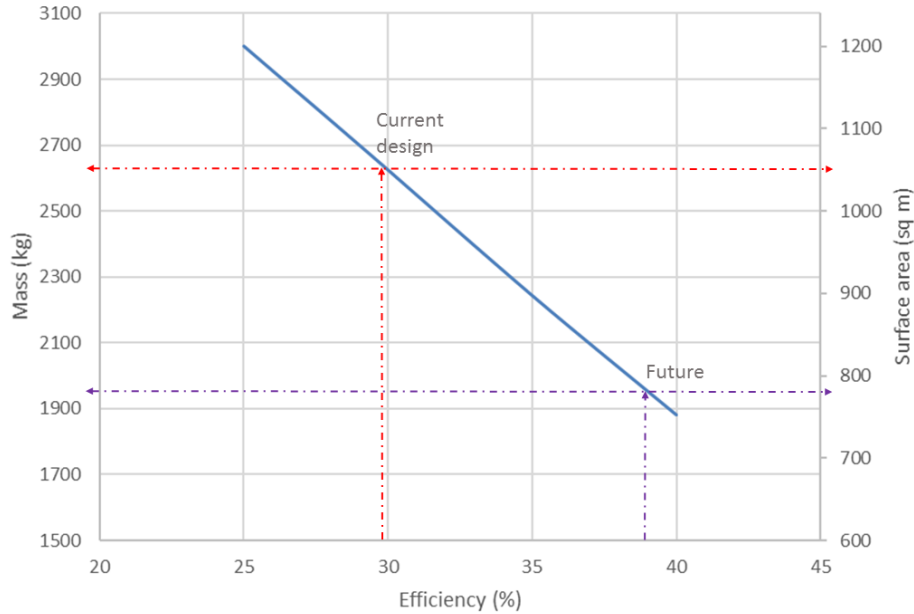


Figure 3: Solar panel configuration for 200 kW (4x50 kW) Tug.

The arrays used will be flexible and able to fold out as an accordion, such as those used in the first Hubble Space Telescope, the Olympus or the ISS. This provides a much lighter option than the rigid alternative and occupy less volume when stowed. However, as they are so thin, they must resist a significant thermal gradient between both sides when exiting an eclipse, this has the potential to cause slight buckling in the array due to the differences in the coefficients of thermal expansion between the solar cells and the substrate [4]. This will cause an estimated 3% loss of power compared to rigid aluminum honeycomb arrays but, the reduction in mass (from 4.5 to 2.5 kg/m²) and volume make flexible arrays the favorable choice. The panels will be deployed using electrical actuators and an expandable truss. During the launch, the arrays and expandable truss will be folded against and stowed inside the solar power module.

The typical layer configuration of the solar arrays, including the cover glass protection, has an estimated degradation of 15% over 15 years in LEO orbits. As the meteoroid impact rate is higher near the Moon [4], a 20% degradation over 15 years has been used. As an example, in a scenario similar than the designed LEO orbit, orbital debris particles up to 0.7 cm in size, and meteoroids up to 0.3 cm in size can be expected to collide with the solar panels.

Exploring future options, using concentrator photovoltaic cells would provide much greater efficiency, reaching values close to 40%. This would decrease the mass and size of the solar arrays below 2000 kg and 800 m² (Figure 6). This technology uses lenses or curved mirrors to focus the sun's rays into the solar cells, usually multi-junction ones, and it is already used on ground provided by many companies, but it has a TRL below 7 in terms of space applications and require greater pointing accuracy.

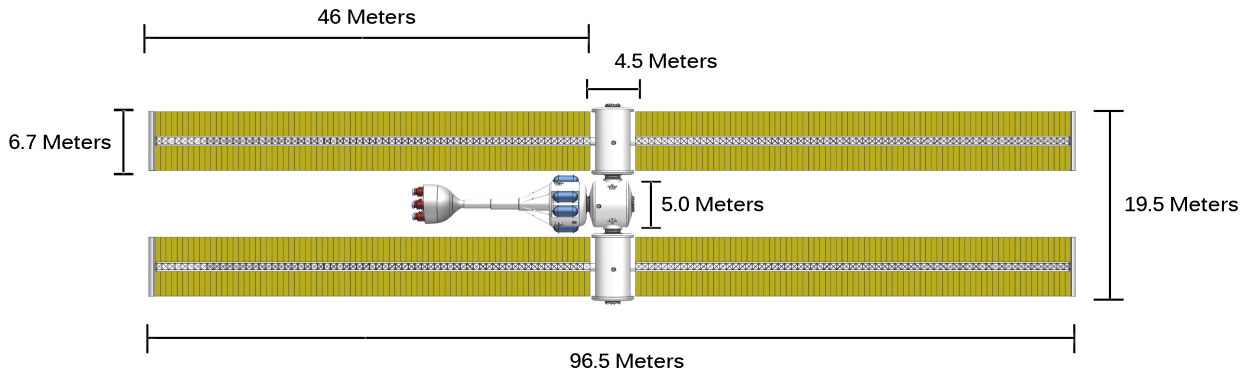


Figure 4: Solar panel configuration for 200 kW (4x50 kW) Tug.

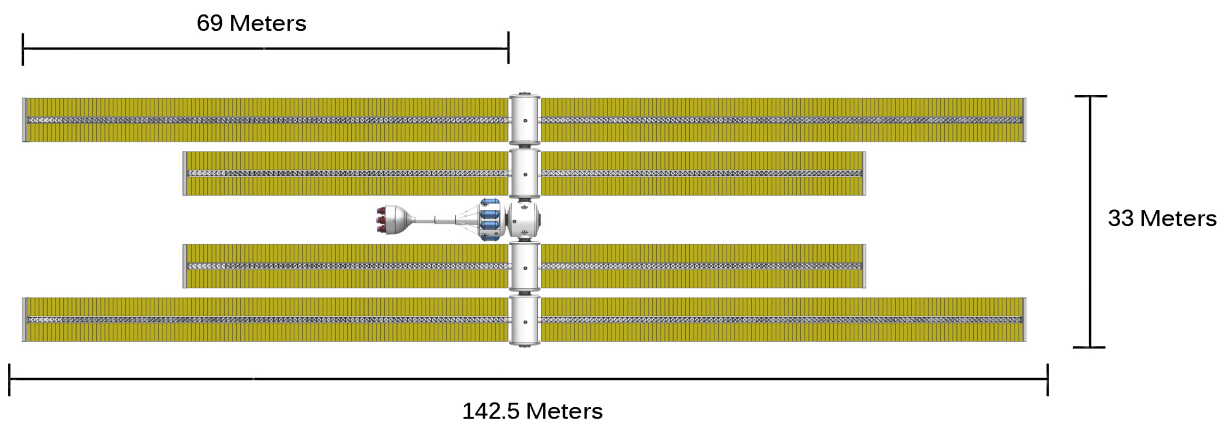


Figure 5: Solar panel configuration for 500 kW (two additional modules carrying 150 kW each) Tug.

2.2 Power and Thermal Systems

The power processing system will incorporate a direct-drive unit (DDU). Direct-drive systems have the advantage of increased efficiency and decrease system mass as compared to conventional systems. For solar electric propulsion engines efficiency goes up by 7% from 92% to 99% percent for direct-drive systems. An increase in thermal efficiency is also seen with direct drive systems as well as a decrease in overall mass as compared to a conventional system. It was determined that the Tug must have on-board power sufficient to supply the Tug with 25% of its overall power needs. In order to avoid carrying parasitic mass, batteries will be housed in each solar panel modules so that power storage capacity increases linearly with solar power. With a calculated eclipse time of approximately 3.4 hours, and using Yardney 43-1 Lithium Ion cells, it was determined that each 100 kW solar panel module will have 58 strings each with 27 cells. Each battery pack will be replaceable and accessible by the robotic arm.

The most important consideration for the thermal subsystem is DDU heat rejection. A maximum temperature of 60°C is allowed due to electronics requirements. A radiator system will be used, operating using liquid ammonia, which has a high thermal capacity and a wide range of operating temperatures. Ammonia loops will collect heat from different subsystems through several tubes and emit it into space through radiators.

The radiator system will be painted white, which in several studies^[5] has been demonstrated to reach a thermal emittance of 0.9 and an absorbance of 0.1. A total surface area of 26 m^2 is required, it will be distributed between two radiators, mounted on the keystone module in order for them to be as close to the DDU as possible. The radiators will be made of aluminum bonded honeycomb

material, and will have a scissor mechanism which will allow for a small package size and the ability to vary length in order to control the temperature of the spacecraft. Each of the radiators will have two independent ammonia loops, physically separated to prevent the collapse of the system by a debris impact.

2.3 Propulsion System

2.3.1 Thruster Selection

There exist several electric thrusters that would in theory provide better performance for the designed mission. In the interest of costs, options were limited to state of the art thrusters that are either flight qualified or have a high enough technology readiness. For example, Magnetoplasmadynamic Thrusters (MPDT) are advantageous for their high thrust and high efficiency at hundreds of kilo-Watts, which falls exactly into our power design range. Pulsed Inductive Thruster (PIT) are also a nice option for their long service life due to their lack of electrodes and ability to employ a variety of propellants, notably carbon dioxide which can be obtained on Mars. However these types of thrusters have limited experimental data from test conducted in a laboratory environment, which make them unlikely considerations for a mission in the near future. Given the vision of this competition to build a simple, durable, and relatively low cost space tug, the use of VASMIR cannot be recommended due to its complex design, manufacturing, and its difficult serviceability, although it has a superior performance in interplanetary flight. Considering that the tug will mainly focus on lunar missions and in the future will implement a large number of tugs, the economic feasibility of design is critical when selecting the propulsion system.

Although Hall Effect Thrusters (HET) relies on much more complicated physics than an ion engine to produce thrust, they actually use a much simpler structure, consisting of a cylindrical channel with an interior anode, a magnetic circuit that generates a primarily radial magnetic field across the channel, and a cathode external to the channel. While HETs typically have lower efficiency and lifetimes than ion thrusters, their advantageous power-to-thrust ratio, which is closely related to mission transfer time, and lower specific mass can offset this weakness and will be discussed in the trajectory analysis.

A traditional HET only has one channel. The Plasmadynamics and Electric Propulsion Laboratory at the University of Michigan and Air Force Research Laboratory have explored an often unheard concept, nesting. The nesting of a thrust involves having more than one discharge channel on a single engine unit. The practice of this concept produced the Nested Hall effect Thruster (NHT) model X2, and a more powerful model X3 that demonstrated powers to 61 kW and is designed to achieve about 200 kW. The footprint area can be decreased by nesting the discharge channel. Therefore, for a high power (hundreds of kW) thruster the mass can be significantly smaller. Remarkably, NHT has the scalability to high power and exceptional throttle-ability based on different configuration of the channels. By adjusting the exit area, i.e. activation of different combination of available channels, the thrust and the Isp can be controlled to have additional flexibility for different mission goals and trajectories. Some configurations are shown above. It has been experimentally tested that NHTs are well suited to missions that require high power supply. Therefore, the model of NHT used as our propulsion thruster is the latest X3, which has been operated for over 11,000 hours. More research are being conducted to test the maximum lifetime under nominal working condition and it is expected to function for 5-10 years after recent modifications.

Each X3 thruster weights around 250 kg and produces 1518 mN at 30 kW and 4000 mN at 100 kW. The efficiency ranges from 50 – 70% with corresponding Isp ranging from 1600 to 4000 seconds. Seven 100 kW X3 NHT will be installed on-board, in a hexagonal configuration with one thruster in the middle. This configuration will account for vertical thrust loads on the launch vehicle, eliminating the need for specialized thrust structure. Having 7 thrusters on-board will allow the Tug to expand to 500 kW while keeping the thrust modules symmetric and also provide redundancy. During nominal

200 kW operation each of the 7 thrusters will be operating at 27 kW utilizing 190 kW of the available 200 kW in order to leave power for the robotic arm, avionics, payload maintenance equipment, and other electronics.

2.4 Main Engine Module

First of all, the engine module is not in direct contact with the keystone module. The reason behind is the potential damage the exhaust plume impingement could damage the surrounding structure, e.g., if the far end of solar panel is too close to the plume region in a certain configuration. Moreover, in addition to the ions that are leaving the thrust, there are also some neutrals that escape without being ionized. These neutrals are slow moving and form a low density cloud behind the thruster. A small fraction of the energetic ions leaving the engine can collide with these neutrals and undergo charge exchange (CEX) resulting in a high velocity neutral and low velocity ion. These low velocity ions can then be captured by the sheath potential and accelerated toward the spacecraft. If the plasma is not neutralized completely, not only the sheath fall can be large enough that the accelerated ions can damage the spacecraft surfaces by sputtering away material, the particle cloud can also affect the signals as electrical noise or reduce the speed of ions shooting out of nozzle.

There are several ways to place the propulsion module further away from other modules, including using the expandable truss, which is recently being developed in various forms. For a space tug that will be expected to function in space for at least fifteen years, high confidence on safety is a necessity to ensure the success of missions, especially for the propulsion module. The power lines and propellant lines are more fragile than other main modules with casing. If expandable truss is utilized, wirings and crucial tubing are exposed to space and at high risk to get damaged from space debris and experience extremely cold and hot temperature in the vacuum. The telescopic boom resolves this issue by encasing the cables. A reflective coating applied to the telescoping boom will also reflect off some light and prevents the internal temperature from getting too high for the electronics and sensors.

As Figure 5 indicates, the telescoping boom is retracted into the tank module when on the ground. The structure on the tank module is capable of sustaining the weight from keystone and other modules. Six small booms are attached to the bottom boom to help retracting, telescoping and with structural support. The telescoping boom not only serves the protection of internal power and electronics, but also a mechanism making replacement of engine module easier. The telescoping boom is a modular component that has built-on rails, solid tubing, valves and servo that ensure the stable connection of engines, without separating the tank module from keystone module. The telescoping boom work as a rigid plug, inserting into the tank module without utilizing a berthing port.

In order to save weight, the thrusters will only employ small gimbals. A lot of freedom to vector the thrust for electrical propulsion is not necessary. This is because the thrust generated by electrical thrusters is too small for stance maneuvering. This mission is optimized to not have abrupt change of thrust vector. Therefore, the reaction control system located on the keystone module will be competent to effectively and efficiently change the thrust direction in a few seconds.

2.4.1 Tank and Propellant Selection

The tank module consists of three revolver hubs and can be equipped with 3 tanks for Cis-Lunar missions or up to 9 tanks for interplanetary missions. Each tank will be held in place by a electrically actuated barrel bolt lock mechanism. The revolver is able to rotate the tanks outward in order to have them replaced by the robotic arm onboard. This enables our system to refuel and expand propellant between missions. For a Cis-Lunar mission, the external tanks would not necessarily be installed if refueling is viable every time the tug returns to LEO. When refueling missions become difficult to schedule, the tug can carry spare fuel tanks for longer period missions, although this decreases flight efficiency.

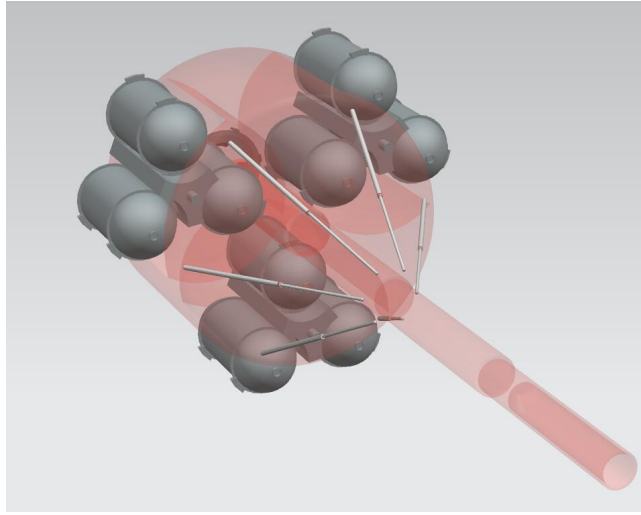


Figure 6: Revolving tank configuration and the central telescoping boom

Some designs have tanks hidden inside compartments. But due to the limited payload space on the launch vehicle, and difficulty of replacement. The tanks shown are partially exposed in the space, and they can revolve around their respective axis to the outside in order to be replaced or expelled. In addition, even if the probability of getting hit by meteoroids are low, the result of such impact is fatal to the mission. Due to the tank is highly pressurized, the propellant would escape through the leakage hole in gaseous form and at high velocity. This momentum would result in additional cold gas thrust, which would be much larger than that from the actual on-board thrusters. It will generate unwanted rotation that will bend the skeleton structure of solar panels, or a velocity vector that is not in the direction of designed trajectory. Hence extra propellant will be wasted to have the space tug to reach the same destination based on a redesigned trajectory. In the event that this happens there is an ejection mechanism for ruptured tanks to limit the propellant lost. This mechanism will also allow us to eject propellant tanks to eliminate parasitic mass of empty tanks during flight in the event of a mission with tight mass margins.

Since the most outside tank on each hub is mostly exposed. This greatly reduces the difficulty for the robotic arm to perform replacement. The tank shall be used is rotated to the inner location where the fuel pipe above the tank hub will autonomously connect to the valve and can be intelligently cut off in emergency as well. The entire tank module is connected to the keystone module. Signals and power can be transferred through the contact pin all the way down to the engine module.

The X3 NHT has operated using two types of propellant: Krypton and Xenon. Xenon is the favored propellant for electrostatic thrusters since it is the heaviest noble gas which is not radioactive. Xenon is not hazardous and does not condense on spacecraft components that are above cryogenic temperatures. Both Krypton and Xenon are easily stored at high densities with low tank mass fractions. The difference between the two types of propellant with respect storage is negligible. However with regard to cost, Xenon is 5-10 times more expensive than Krypton. The performance of Krypton in the thruster is significantly lower than that of Xenon and will increase overall propellant mass [7]. If the price of Xenon does not dramatically increases in the future it will be used. The fuel pipeline is inside the truss/boom structure it is shielded along the main structure from the propulsion module to the tank module. A number of tanks, based on the mission budget, can be externally attached to designated fittings along the truss member with the robotic arm on-board.

2.4.2 Lifetime Analysis

The Nested HET so far has only been tested over 10,000 hrs to ensure the minimum lifetime. Laboratory teams are expecting 50,000 hrs. With modularity and easy replacement features, it is still promising but needs to be tested thoroughly.

2.5 Metrology System

For the longer range navigation necessary for assembly, payload delivery, and refueling each module and payload will contain four radio beacons, communicating via both the X and Ka bands, which will allow for the target module or payload to relay their position and velocity relative to the keystone chaser module with one extra beacon for redundancy. In addition to this the keystone module will be equipped with a star scanner in order to provide a backup system which is able convey its ephemeral data to other spacecraft in the event of an emergency. Once the target module is within 2000 meters an on-board TriDar system, which utilizes both LiDar and 3D laser triangular, will be used for more accurate position and velocity computations. Due to the fusion of both 3D laser triangulation cameras and LiDar, the TriDar system will provide accurate position and velocity data until the target module is within 5 meters. In the 100 meter range the TriDar system is advertised to provides positional accuracy within ± 100 cm, orientation accuracy of $\pm 10^\circ$, and a refresh rate of 1 Hz. At the 20 meter range the TriDar system is advertised to provides positional accuracy within ± 30 cm, orientation accuracy of $\pm 3^\circ$, and a refresh rate of 5 Hz. Once the target module is within the five meter berthing box, a high resolution camera will be used, in combination with fiducial markings, in order for the robotic arm to grasp the grapple fixture of the target.

2.6 Robotic Arm

A robotic arm will be on-board the tug to assist with the assembly as well as to replace propellant tanks and batteries. It's design has been modeled off of the CandaArm2 being used on the International Space Station, the only change is that it has been scaled down to 12 meters in total length. The arm contains two wrist joints, each with 2 degrees of freedom, and one elbow joint with three degrees of freedom. It is symmetric about its length and thus each wrist joint contains an end-effector which is able to grasp the standard grapple fixture. Each module has two of these for structural transportation which can transfer power and data, enabling the arm to move between modules. The batteries and propellant tanks also contain grapple fixtures which do not have power and data transfer capabilities but allow component to be installed and uninstalled. This will allow us to refuel, add additional tanks for range extension, remove the parasitic mass of unused propellant tanks during flight, and replace batteries as they will expire before a majority of the Tug's other components.

The algorithm described in Figure 7 the general logic is described for the robotic arm will be capable of autonomous operation during missions to Low Martian Orbit. Arm movements will be decided by a choosing function over all possible actions. A trained movement planner will generate collision free actuation paths considering operation time, and RCS propellant and electrical power consumption. With multi-level sensor system, the measurement error should be able to be controlled within the range of ± 1 cm in position, $\pm 0.5^\circ$ in rotation, ± 2 mm/s in velocity and 0.01° /s in rotational speed. The robotic arm should be able to perform the desired tasks with an expected same accuracy in rotational speed and higher accuracy in linear velocity compared to the original CanadArm2 as it has the same actuators however, is shorter in length.

2.7 Connecting Mechanism

The connecting mechanism which will be used is based around the common berthing mechanism. There will be external power and data connections running between the modules. In the case of the solar power modules the berthing mechanism will lie on a geared, motorized ball bearing which will allow the modules to be rotated. This will require electrical slip rings in order to maintain power and data connections. Each connection will be contain a large number of vibration isolators which will serve to decrease lateral and vertical responses to any oscillations.

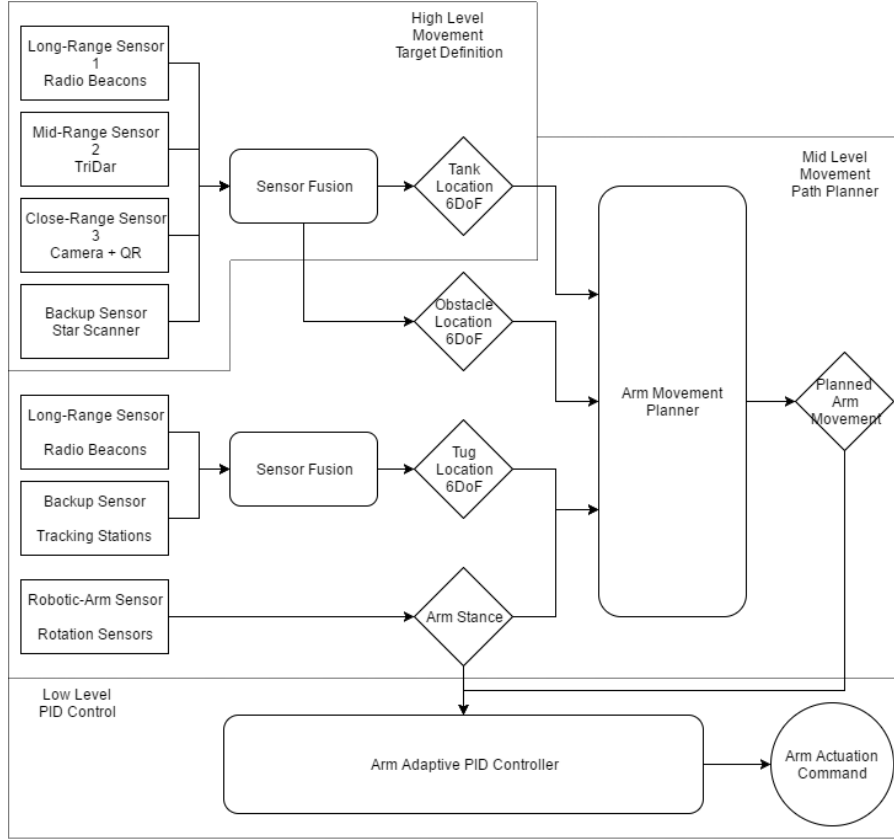


Figure 7: Robotic Arm Control Flow Chart

3 Concept of Operations

Figure 8 shows that, while counterintuitive, higher thrust will increase the mission time. Due to higher mass flow rate needed to conduct high thrust exhaust the propellant required to be carried on board will rapidly increase resulting in a slower transfer time. The first pass analysis was based on pure Tsiolkovsky rocket equation. This time, methods with higher order of accuracy is employed to visualize the trajectory.

A 3D trajectory simulation has been developed and performed in MATLAB to get a more accurate result. β is the initial out-of-plane thrust vector. Δi is the total inclination change from the initial circular orbit to the final circular orbit plane. the total Δv can be calculated via Equation 1. Equation 2 will give the initial thrust yaw angle β_0 . The relationship between propagation time, initial and final radius, initial and final velocity can be found from Equations (3) to (5). The out-of-plane thrust yaw vector, which is a function of time t . The result is optimized to have the vehicle reaching designated radius as inclination change is reached at the same time.

$$\Delta v = v_0 \cdot \cos \beta_0 - \frac{v_0 \cdot \sin \beta_0}{\tan \left(\frac{\pi}{2} \Delta i + \beta_0 \right)} \quad (1)$$

$$\tan \beta_0 = \frac{\sin \left(\frac{\pi}{2} \Delta i \right)}{\frac{v_0}{v_f} - \cos \left(\frac{\pi}{2} \Delta i \right)} \quad (2)$$

$$v_0 = \sqrt{\frac{\mu}{r_0}} \quad (3)$$

$$v_f = \sqrt{\frac{\mu}{r_f}} \quad (4)$$

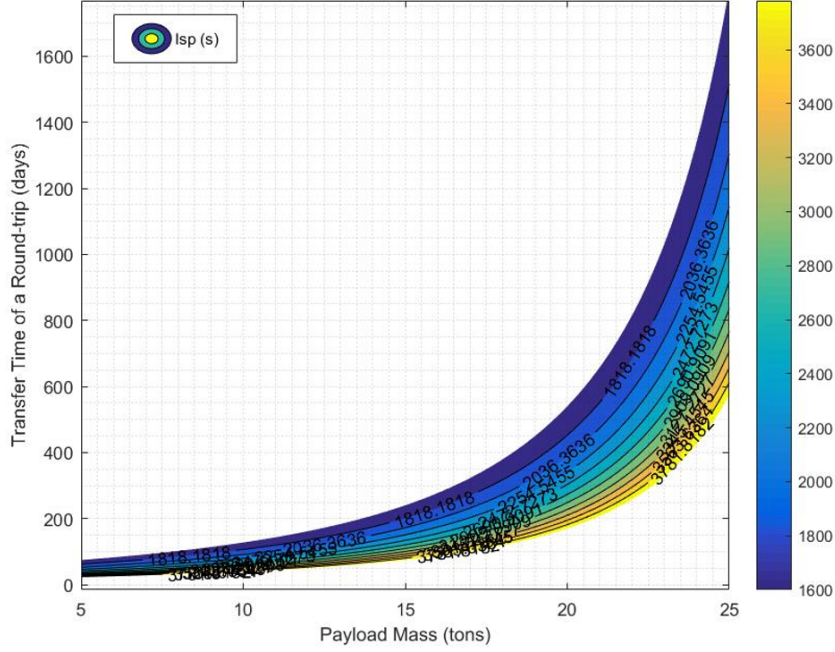


Figure 8: Roundtrip Time vs. Payload Mass vs. ISP

$$\beta(t) = \tan^{-1} \left(\frac{v_0 \cdot \sin \beta_0}{v_0 \cos \beta_0 - a_T t} \right) \quad (5)$$

Since the thrust is constant and continuous, Equation 6 is combined acceleration of gravitational pull and thrust. If the thrust T is in the same direction of the velocity vector, another form of is shown also in Equation 6, which has a first order and second order term, making the system easier to solve. Incorporating with the rocket equation, equations 6 and 7 can be written in 2nd order linear differential equation form in order to be solved numerically. By rearrange the terms, we have the Equation set 9. The vector y consists of three position vectors and three velocity vectors, which can later be visualized to demonstrate the trajectory. Runge-Kutta-Fehlberg method is employed to solve the equation set.

$$P = \frac{T g_0 I_{sp}}{2\eta} \quad (6)$$

$$\ddot{\vec{r}} = -\mu \frac{\vec{r}}{r^3} + \frac{\vec{F}}{m} = -\mu \frac{\vec{r}}{r^3} + \frac{T \vec{v}}{m v} \quad (7)$$

$$\frac{dm}{dt} = -\frac{T}{I_{sp} g_0} \quad (8)$$

$$\dot{\vec{y}} = \vec{f}(t, \vec{y}) \quad (9)$$

$$y = \begin{Bmatrix} x \\ y \\ z \\ \dot{x} \\ \dot{y} \\ \dot{z} \\ m \end{Bmatrix} \dot{y} = \begin{Bmatrix} \dot{x} \\ \dot{y} \\ \dot{z} \\ \ddot{x} \\ \ddot{y} \\ \ddot{z} \\ \dot{m} \end{Bmatrix} \begin{Bmatrix} y_4 \\ y_5 \\ y_6 \\ -\mu \frac{y_1}{r^3} + \frac{T}{m} \frac{y_4}{v} \\ -\mu \frac{y_2}{r^3} + \frac{T}{m} \frac{y_5}{v} \\ -\mu \frac{y_3}{r^3} + \frac{T}{m} \frac{y_6}{v} \\ -\frac{T}{I_{sp} g_0} \end{Bmatrix} \quad (10)$$

When the tug is approaching the Moon, the velocity it travels at becomes closer to the parabolic velocity. This means the orbit will less spiral and more elliptical. When the tug flies into the Moon's

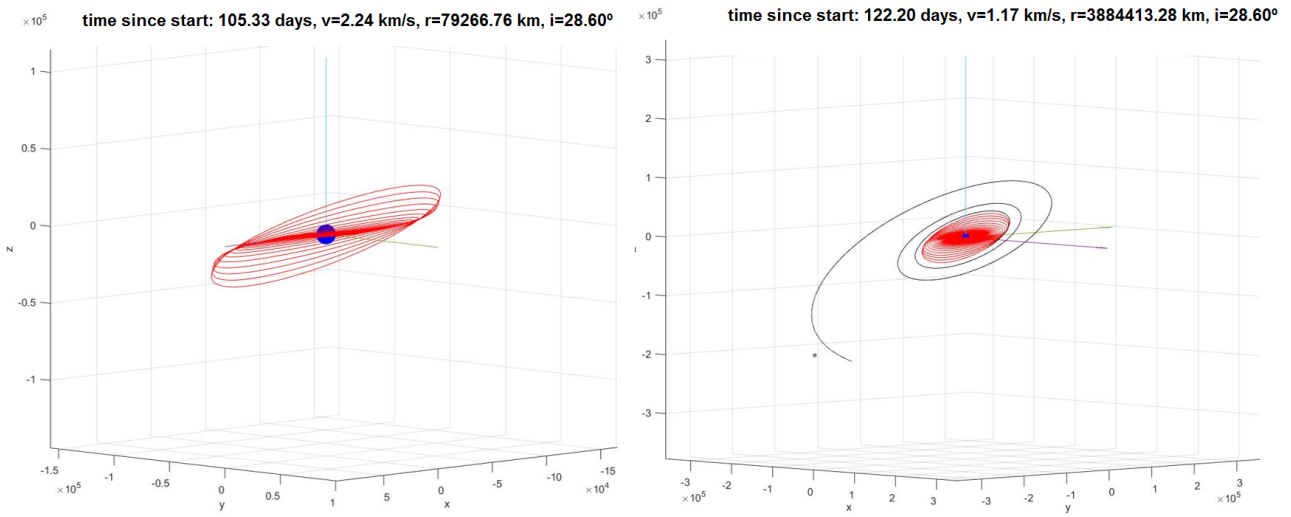


Figure 9: Left: First phase of trajectory - changing inclination to the Moon's orbital plane. Right: Second phase of trajectory - reaching to the Moon's sphere of influence

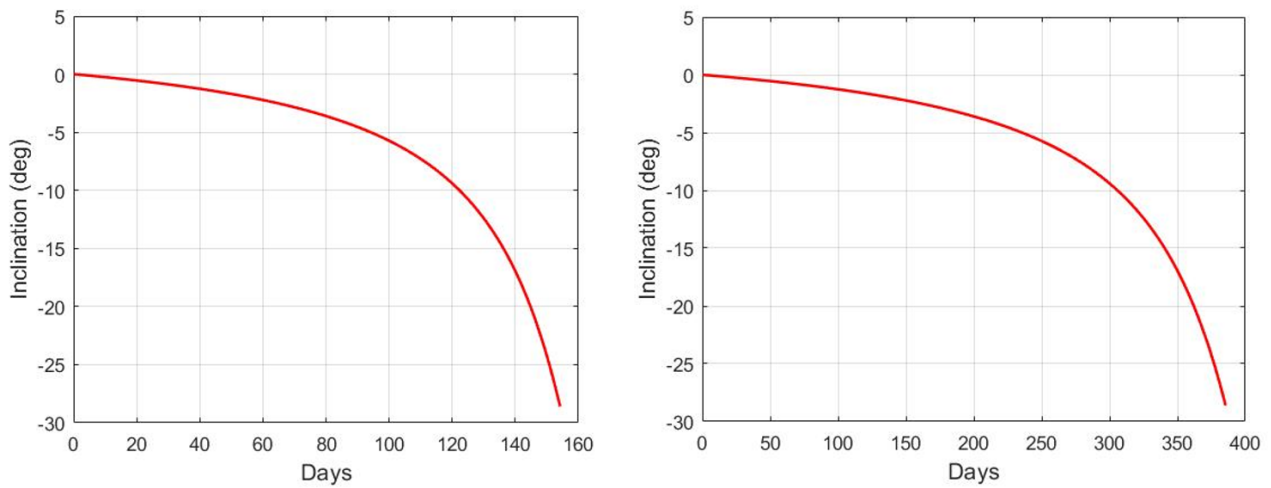


Figure 10: Inclination for 10 MT (left) and 20 MT (right) mission. Both reach target radius at the same time as they reach the maximum inclination

SOI, the orbit around the moon will be highly elliptical as well, or might not be small enough to be captured by the Moon's gravity. If the orbit around the Moon is elliptical, it will be highly time consuming and propellant wasting to circularize and elevate the orbit to LDRO. Therefore, the best way is to start the mission in a specific launch window so that the tug will tangentially intercept with Moon's SOI at the right velocity. Based on patched conics assumption, the tug can then be seen as immediately orbiting the Moon in a circular orbit. For example, this result is based on the assumption of 10,000 kg overall mass, and 170 kW available power for the NHT thrusters, Isp equals to 4000s with 60% efficiency. The algorithm will work with different systems and masses. As result, the Moon needs to be 105.56° of true anomaly ahead of the space tug in order to have interception with the Moon's SOI at 90° and at the right speed for a circular lunar orbit. The whole transfer costs 122.2 days and the return trip to LEO will be less time. Below are the figures for comparing inclination vs. mission period for a 10 MT system and 20 MT system.



Figure 11: Assembly of one of the solar panels module

3.1 Launch Packaging

The first launch will be sent to LEO using the United Launch Alliance Delta IV M+(4,2) as the long fairing can fit the keystone module while it is attached to the propulsion module loaded with propellant. This will result in a total payload mass of 10MT which the Delta IV M+(4,2) is capable of delivering to LEO. The package will be arranged in the fairing as Figure depicts.

The second and third launches will utilize the Falcon 9 rocket with each containing a solar power module, as the following figure depicts. Two Falcon 9 launches were chosen to carry the two solar power modules rather than a single Delta IV as they are both light enough and small enough to fit. Launching two separate Falcon 9s is more economical and eliminates the need for a complex separating mechanism when deploying the solar power modules from the fairing when compared with a single Delta IV.

3.2 On-Orbit Assembly

The first launch containing the keystone module, propulsion module, and propellant module will take approximately 2.3 hours to get to Low Earth Orbit according to the Delta IV User's Guide. This will result in a 300 km orbit with a tolerance of ± 11 km. After 48 hours of flight pad refurbishment the second launch containing the first solar power module will be sent to the orbit at which the keystone module ends up. This will approximately take another 2.3 hours. The keystone module will then conduct an R-Bar rendezvous approach to bring the solar power module within the berthing box. The worst case scenario for the second launch is that it ends up in an orbit 11 kilometers greater or lesser than the orbit of the keystone module. This worst case scenario will result in a total rendezvous time of 5 hours provided the launch timing is coordinated with the phasing of the keystone module's orbit. Once the solar power module is within the berthing box it will take approximately 3 hours for the robotic arm to grasp the solar power module and bring the berthing mechanism into their bolting position based upon the time required for the same operation between the ISS and a Dragon capsule. The bolting process will then begin. The process begins with the active ring capturing the passive ring. Then the initial "A-bolt operation" brings 2 rings together and applies 1500 pounds of preload, this will take approximately 30 min. The arm then separates and goes to the ready position. Bolt activity must then be halted 12 hours for thermal equalization. Next, the "I-bolt operation" 4 bolts

are driven at 0.6 RPM in 5 stages, this takes an additional 30 minutes. Then, two bolts are driven diagonally opposing on the ring, and two more bolts are driven at 90°, this goes around for all 16 bolts to preloads in five stages until it reaches 10,500lbs, taking a total of 30 minutes. The process is again halted for thermal for 12 hours. Finally the “F-bolt” level, maximum drive power preloads are achieved in the same sequence as the ”I-bolt” reaching 19,300lb preloads, taking 30 minutes. The total time for the bolting procedures is expected to be 26 hours. After the second launch a third is sent up containing the second solar power module after a launch pad refurbishment time of 48 hours. The same process and time line for rendezvous and berthing is used for the second solar power module as was used for the first. This result in a total mission-time of 5.8 days, an overview of the assembly timeline is given in Table 2.

Event	Mission Elapsed Time
Launch 1 Liftoff	000:00:00.00
Launch 1 Arrives in LEO	002:30:00.00
Launch 2 Liftoff	050:30:00.00
Launch 2 Arrives in LEO	053:00:00.00
Keystone completes R-Bar rendezvous bringing SP module into berthing box	058:00:00.00
Robotic arm grabs SP module and begins berthing	061:00:00.00
Berthing mechanisms bolted	087:00:00.00
Launch 3 Liftoff	101:00:00.00
Launch 3 Arrives in LEO	103:30:00.00
Keystone completes R-Bar rendezvous bringing SP Module into berthing box	108:30:00.00
Robotic arm grabs SP module and begins berthing	111:30:00.00
Berthing mechanisms bolted	137:30:00.00

Table 2: Assembly Timeline

3.3 Reference Mission

The design reference mission for our SEP tug developed in this paper proposes to bring payloads both to LDRO while in the 200 kW configuration and to LMO in the 500 kW configuration. For LEO to LDRO an in depth analysis has been conducted and as the figure below shows, it will take 380 days and 4 MT of propellant to deliver a 20 MT payload to lunar orbit.

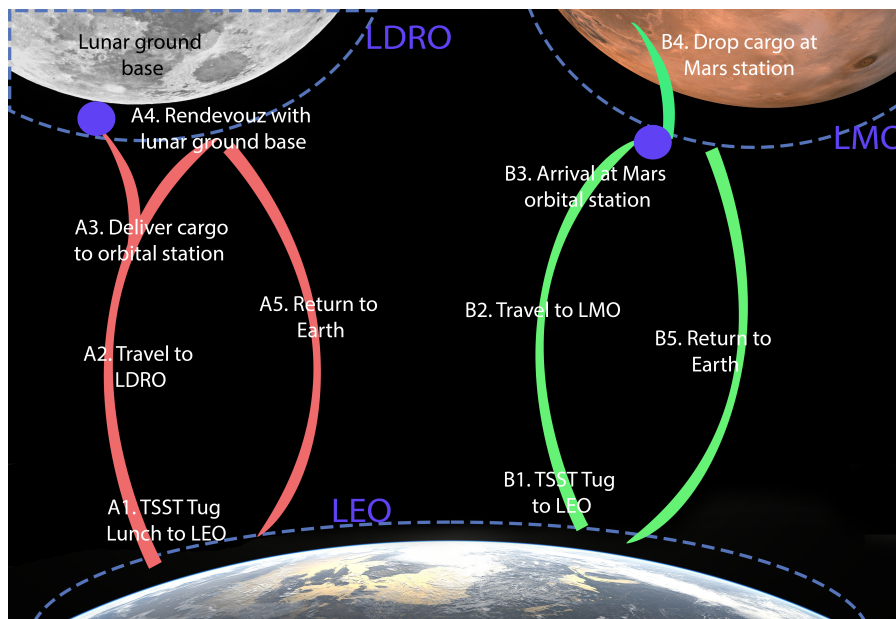


Figure 12: Reference mission.

4 Conclusion

4.1 Low TRL Items

In order to keep costs low, we have elected to utilize higher TRL options whenever possible. However, the nature of designing a reusable, repairable and modular space Tug demands that emerging technologies be utilized, and existing technologies be adapted. The major components of our Tug which have yet to achieve a $TRL > 7$ are the Nested-Channel Hall Effect Thrusters, the Direct Drive Power Units, and automation of a robotic arm to complete tasks such as transferring propellant tanks.

Nested-Channel Hall Effect Thrusters have a relatively high technology readiness level, when extensive laboratory testing has been taken into account. They also share much of their design with traditional low power Hall Effect Thrusters. The combination of these two factors make it reasonable to expect these thrusters to achieve a technology readiness level suitable for use within the next few years. The direct drive power units are surprisingly complex and as time estimates to develop traditional power processing units, let alone state of the art direct drive units, is commonly underestimated it is imperative that this item undergoes extensive testing and development prior to its use in such a high powered system. Recent tests using a direct drive power system with high powered hall effect thruster by GRC and JPL researches [12] demonstrates the possibility of a direct drive power processing unit however, scaling a power processing unit from the 12.5 kW thruster tested to seven 100 kW will prove a challenge. To overcome this challenge extensive development and experimental testing will be required.

The automation of a robotic arm to transfer propellant tanks and complete various maintenance tasks has been done for Earth-based applications but has not yet been applied in deep space. Testing of this system in a neutral buoyancy tank such as at the Neutral Buoyancy Research Facility on the University of Maryland campus will be required in order to develop and test an algorithm that will allow the arm to perform required tasks. The wide spread use of robots to perform complex tasks instills confidence that a robotic arm will be able to perform a similar task in space given enough testing and development. As the tanks will be delivered by a vehicle which docks to the Tug, the tanks will be in a known and fixed location relative to the robotic arm which will greatly simplify the initial maneuver of grasping the tanks. Utilization of ground testing to automate robotic tasks typically done using telerobotics will reduce the expense associated with human involvement of the assembly and maintenance of our Tug.

4.1.1 Looking Forward

The dream of long term space exploration demands the development of an economically efficient method for transporting payloads to various destinations within our solar system. Reusable solar electric propulsion tugs provide a solution to this problem. By using on orbit robotic assembly and refueling our team from the University of Maryland have designed a reusable Tug which is expandable from 200 kW to 500 kW and can efficiently transfer payloads from LEO to LDRO, LMO, and beyond. The design opens the door for further manned and robotic exploration of the solar system and beyond. Looking forward the authors intend to conduct testing to raise the TRL of autonomous berthing and thereby expedite the development time for a solar electric propulsion space tug.

References

- [1] Dick, B., *Current Status of the Nitrogen Oxygen Recharge System*. NASA Technical Report Server. NASA. Web. 2011.
- [2] Heineman Jr., W., *Mass Estimation and Forecasting for Aerospace Vehicles Based on Historical Data*. NASA JSC-26098, November 1994
- [3] Hofer, R.R., Randolph, T.M., *Mass and Cost Model for Selecting Thruster Size in Electric Propulsion Systems*. Jet Propulsion Laboratory, California Institute of Technology, January-February 2013
- [4] Patel, Mukund R. *Spacecraft power systems*. CRC press, 2004.
- [5] *Spacecraft Thermal Control and Conductive Paints/Coatings and Services Catalog*. AZ Technology, Inc., January 2008
- [6] Hall, S.J., Cusson, S.E., Gallimore, A.D., *30-kW Performance of a 100-kW Class Nested-Channel Hall Thruster*. IEPC 2015-125 , 34th International Electric Propulsion Conference, Kobe, Japan, July 6-10, 2015
- [7] Nakles, M.R., Hargus, W.A., Delgado, J. J., Corey, R.L., *A Performance Comparison of Xenon and Krypton Propellant on an SPT-100 Hall Thruster*. Presented at the 32nd International Electric Propulsion Conference, Weisbaden, Germany September 11–15, 2011
- [8] Lobbia, R., *PEPL: Thrusters: X3*. Retrieved from <http://pepl.engin.umich.edu/thrusters/X3.html>
- [9] Florenz, R., Hall, S., Gallimore, A., Kamhawi, H., Griffiths, C., Brown, D., Hofer, R., Polk, J., *First Firing of a 100-kW Nested-channel Hall Thruster*. IEPC-2013-394, 33rd International Electric Propulsion Conference, Washington, D.C., October 6-10, 2013.
- [10] Goebel, Dan M., and Ira Katz. *Fundamentals of electric propulsion: ion and Hall thrusters*. Vol. 1. John Wiley & Sons, 2008.
- [11] Florenz, R., Gallimore, A. D., Peterson, P. Y., *Developmental status of a 100-kW class laboratory nested channel hall thruster*. 32nd International Electric Propulsion Conference. IEPC-2011-246. 2011.
- [12] *Typical Delta V (velocity Increment) Value(s) for Various Space Maneuvers*. Delft University of Technology. Retrieved from <http://www.lr.tudelft.nl/?id=29271&L=1>
- [13] Pinero, L., Scheidegger, R., Bozak, K., Birchenough, A., *Development of High-Power Hall Thruster Power Processing Units at NASA GRC*. 51st AIAA/SAE/ASEE Joint Propulsion Conference (2015): n. pag. NASA Technical Report Server. NASA, 27 July 2015.
- [14] *Dragon C2/3 Mission Timeline*. n.d. Retrieved February 04, 2017, from <http://www.spaceflight101.net/dragon-c23-mission-timeline.html>
- [15] Grunwald, A. J., Ellis, S. R. (January - February 1993). *Visual Display Aid for Orbital Maneuvering: Design Considerations*. Journal of Guidance, Control, and Dynamics, 16(1), 1-6. Retrieved February 3, 2017
- [16] Pasquale, E. D. (2012). *ATV Jules Verne: a Step by Step Approach for In- Orbit Demonstration of New Rendezvous Technologies*. SpaceOps 2012 Conference. doi:10.2514/6.2012-1314619
- [17] Dunbar, B. (2013, January 08). *Canadarm2 and the Mobile Servicing System*. Retrieved February 05, 2017, <http://www.nasa.gov/missionpages/station/structure/elements/mss.html>
- [18] Lee, J., Chang, P., & Gweon, D. (2012). *A cost function inspired by human arms movement for a bimanual robotic machining*. 2012 IEEE International Conference on Robotics and Automation. doi:10.1109/icra.2012.6224643

- [19] Savsani, P., Jhala, R. L., & Savsani, V. J. (2013). *Optimized trajectory planning of a robotic arm using teaching learning based optimization (TLBO) and artificial bee colony (ABC) optimization techniques*. 2013 IEEE International Systems Conference (SysCon). doi:10.1109/syscon.2013.6549910
- [20] C. Yang, H. Ma, M. Fu and A. M. Smith, *Optimized model reference adaptive motion control of robot arms with finite time tracking*, Proceedings of the 31st Chinese Control Conference, Hefei, 2012, pp. 4356-4360.
- [21] Dupuis, E. (2011). *An Overview Of Canadian Space Robotics Activities. Field Robotics*. doi:10.1142/9789814374286_0117
- [22] Weiss, A., Baldwin, M., Erwin, R. S., & Kolmanovsky, I. (2015). *Model Predictive Control for Spacecraft Rendezvous and Docking: Strategies for Handling Constraints and Case Studies*. IEEE Transactions on Control Systems Technology, 23(4), 1638-1647. doi:10.1109/tcst.2014.2379639
- [23] *Proc. of IEEE/RSJ IROS 2005 Workshop on Robot Vision for Space Application*, Shaw Conference Centr, Edmonton, Alberta, Canada. N.p.: n.p., 1993. 1-41. Web. <https://webdocs.cs.ualberta.ca/~robvis05/ProceedingsCompr.pdf>.
- [24] Chung, Emily. *Spacecraft to use Canadian guidance system as 'eyes' on way to ISS*. CBCnews. CBC/Radio Canada, 11 July 2014. Web. 06 Feb. 2017.
- [25] *International Space Station Structures Mechanisms*. Structures and Mechanisms. 05 Feb. 2017. http://pages.erau.edu/~ericksol/projects/issa/s_m.html#mechCBM.
- [26] *European Docking System for the IS*. Internat Ional Berthing Docking MechanI sM (IBDM). N.p.: European Docking System for the IS, n.d. ESA. Web.
- [27] McLaughlin, R. J., & Warr, W. H. (2001). *The Common Berthing Mechanism (CBM) for International Space Station*. SAE Technical Paper Series. doi:10.4271/2001-01-2435
- [28] *Reformulation of Edelbaum's Low-Thrust Transfer Problem Using Optimal Control Theory*, Jean Albert Kechichian, JOURNAL OF GUIDANCE, CONTROL, AND DYNAMICS Vol. 20, No. 5, September–October 1997
- [29] *Orbital Mechanics for Engineering Students*, 3rd Edition, Howard D. Curtis